SUPPLEMENTARY FIGURES

Supplementary Figure 1.1

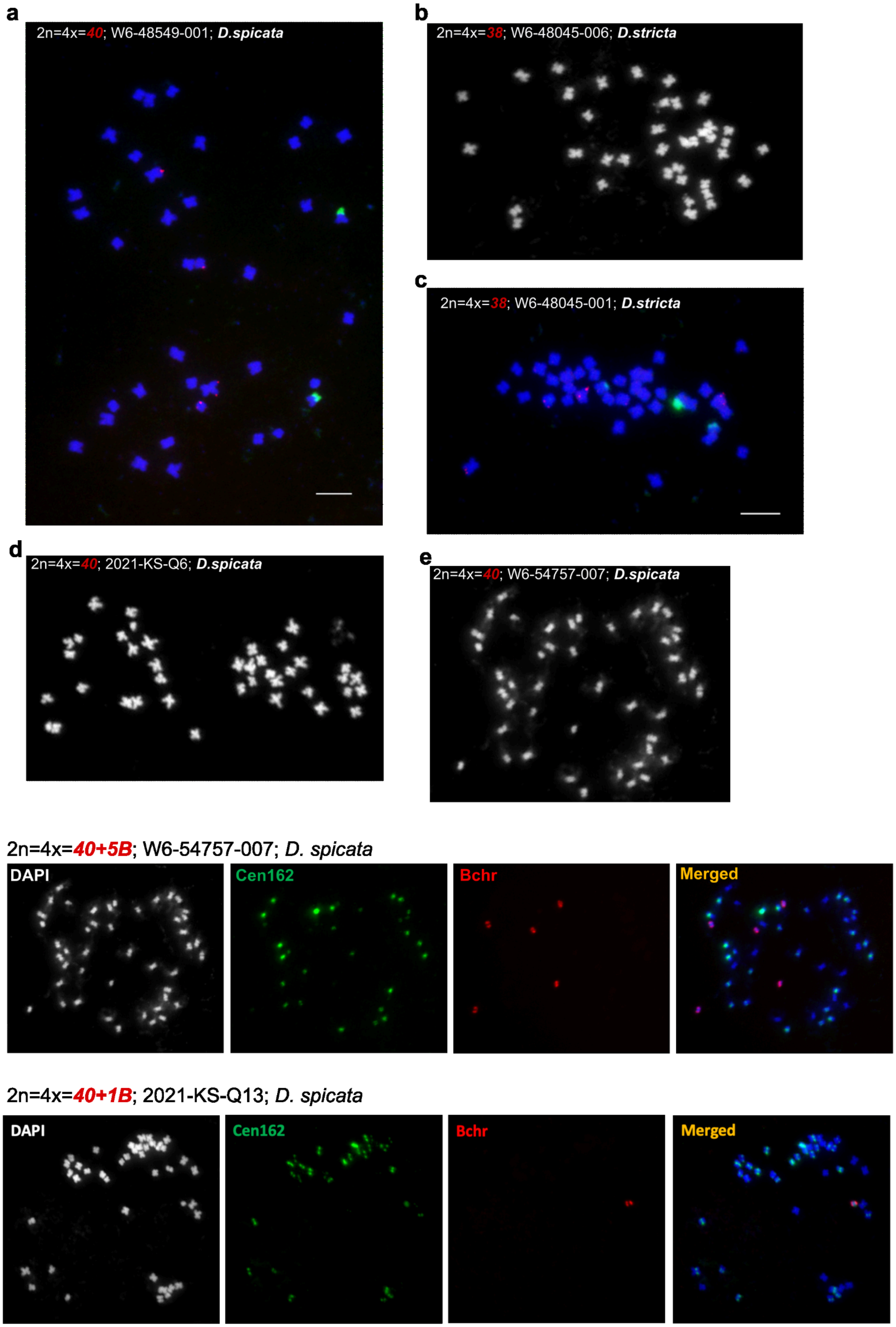

Supplementary Figure 1.1: DAPI stained chromosomes from **a,** W6-48549-001; 2n=4x=40; *D. spicata*, **b,** W6-48045-006; 2n=4x=38; *D. stricta*, **c,** W6-48045-001; 2n=4x=38; *D. stricta*, **d,** 2021-KS-Q6; 2n=4x=40; *D. spicata*, **e,** W6-54757-007; 2n=4x=40; *D. spicata*, **f,** W6-54757-007; 2n=4x=40+5B; *D. spicata* and **g,** 2021-KS-Q13; 2n=4x=40+1B; *D. spicata*. **f** and **g** showing the CEN162 (green) and chromosome B (red) FISH for W6-54757-007 and 2021-KS-Q13, respectively.

Supplementary Figure 1.2

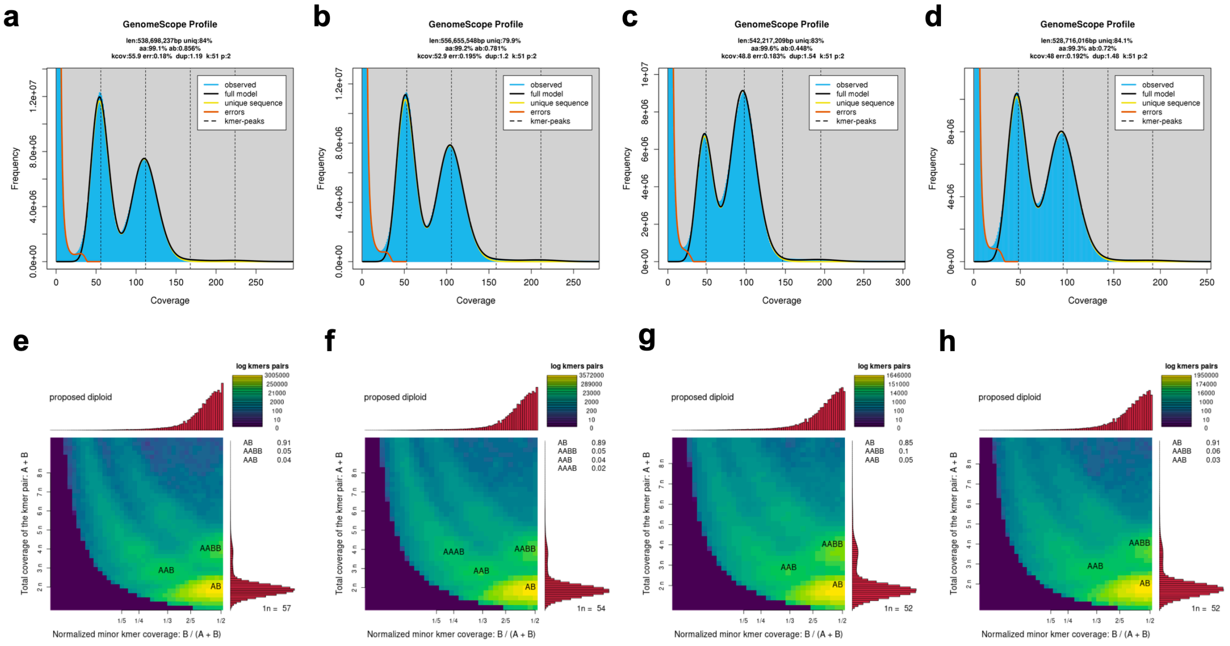

W6-48549-006 **W6-48045-006** **W6-54757-002** **2021-KS-Q6**

Supplementary Figure 1.2: In the initial analysis, k-mer profiles were generated using High-Fidelity (HiFi) reads from W6-48549-006, W6-48045-006, W6-54757-002, and 2021-KS-Q6. All four genomes exhibit a diploid configuration, characterized by a notable level of heterozygosity. Genomescope2 plots (**a-d**) provided predictive insights into various genomic parameters including genome length, uniqueness, and the percentage of heterozygosity. The Smudgeplot analysis (**e-h**) provided an assessment of k-mer coverage, represented by the B/(A+B) ratio. The primary peak, highlighted in yellow, indicates the highest k-mer coverage supporting the AB ratio, confirming a diploid structure. Additionally, a smaller secondary peak, representing the AABB ratio, with lower k-mer coverage, suggests the presence of two distinct subgenomes within the analyzed genomes.

Supplementary Figure 1.3

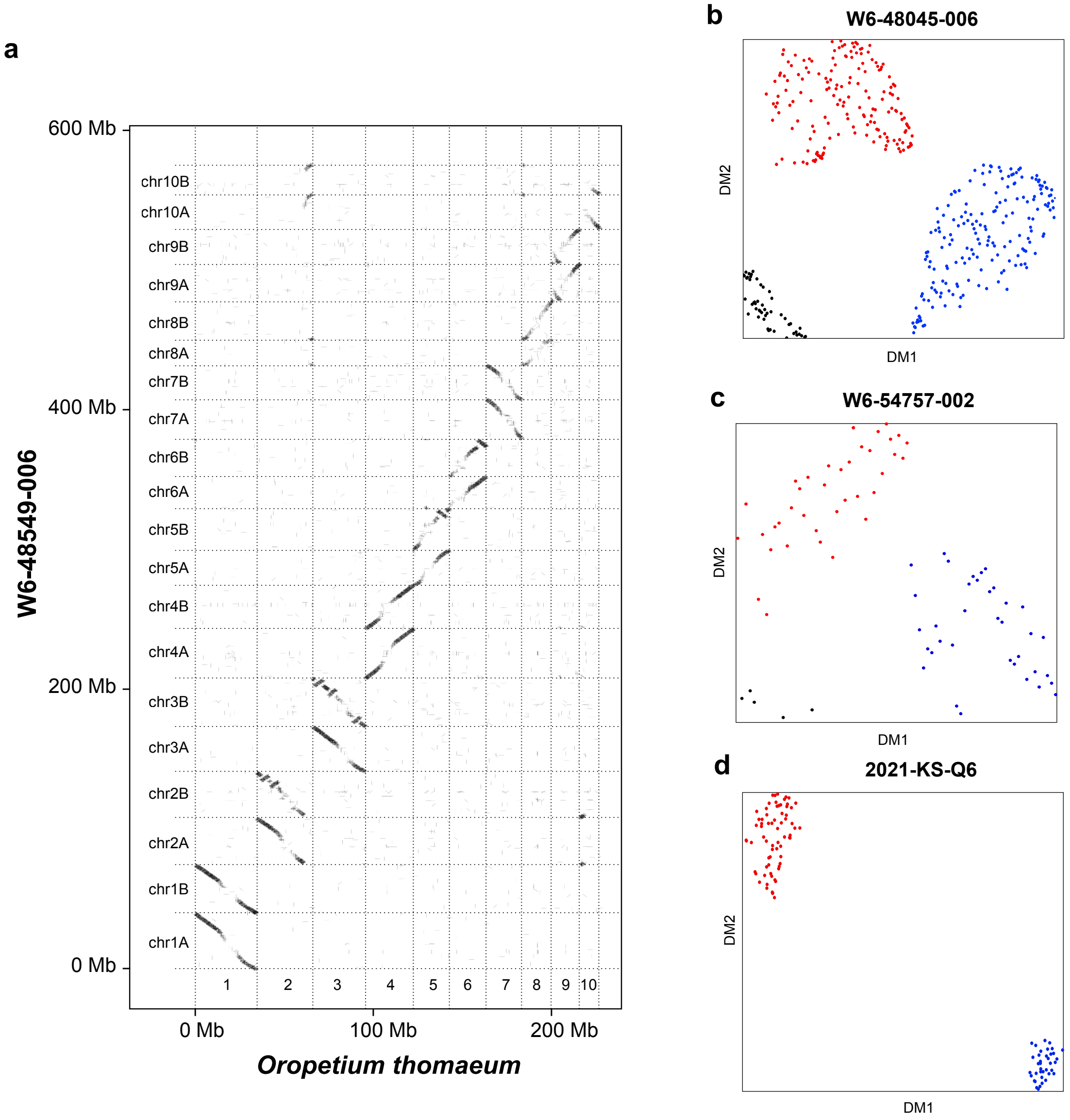

Supplementary Figure 1.3: **a,** Chromosome-level alignments of the final T2T assembly of W6-48549-006 saltgrass genotypes against *Oropetium thomaeum*. The figure illustrates the end-to-end alignment of each chromosome of *O. thomaeum* against two chromosomes of saltgrass, demonstrating its two subgenomes. Subgenome separation is based on TE clustering, showing division into two groups in (**b**) W6-48045-006 (*D. stricta*), (**c**) W6-54757-002 (*D. spicata*), and (**d**) 2021-KS-Q6 (*D. spicata*).

Supplementary Figure 1.4

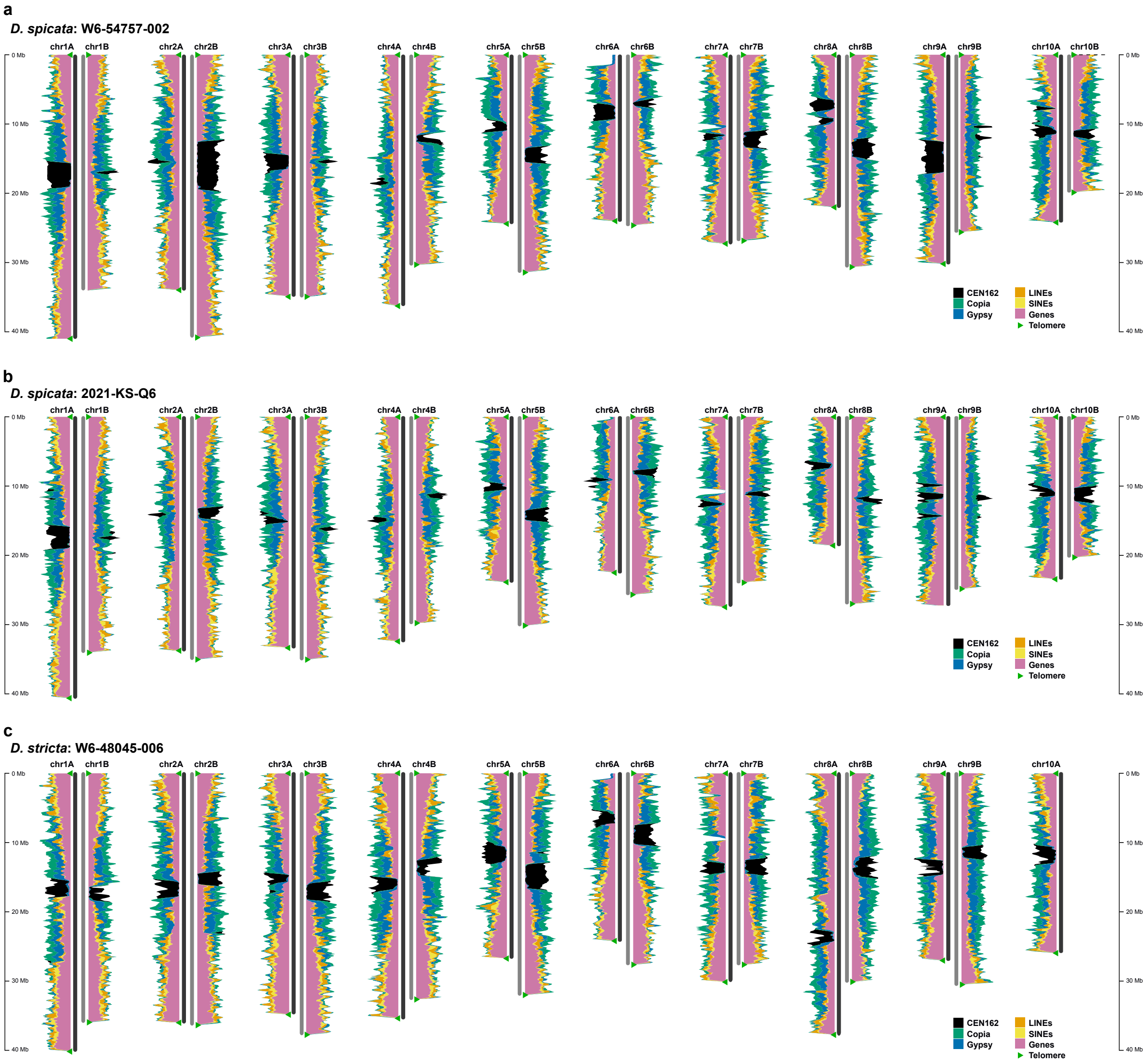

Supplementary Figure 1.4: Distribution of telomeres, CEN162, *Copia* and *Gypsy* retrotransposons, LINEs (Long Interspersed Nuclear Elements), SINEs (Short Interspersed Nuclear Elements), and protein-coding genes across each chromosome of *D. spicata*; **a,** W6-54757-002 and **b,** 2021-KS-Q6, and *D. stricta*; **c,** W6-48045-006. This illustration highlights the spatial arrangement of these genetic elements, providing insights into the chromosomal organization and genome structure of saltgrass.

Supplementary Figure 1.5

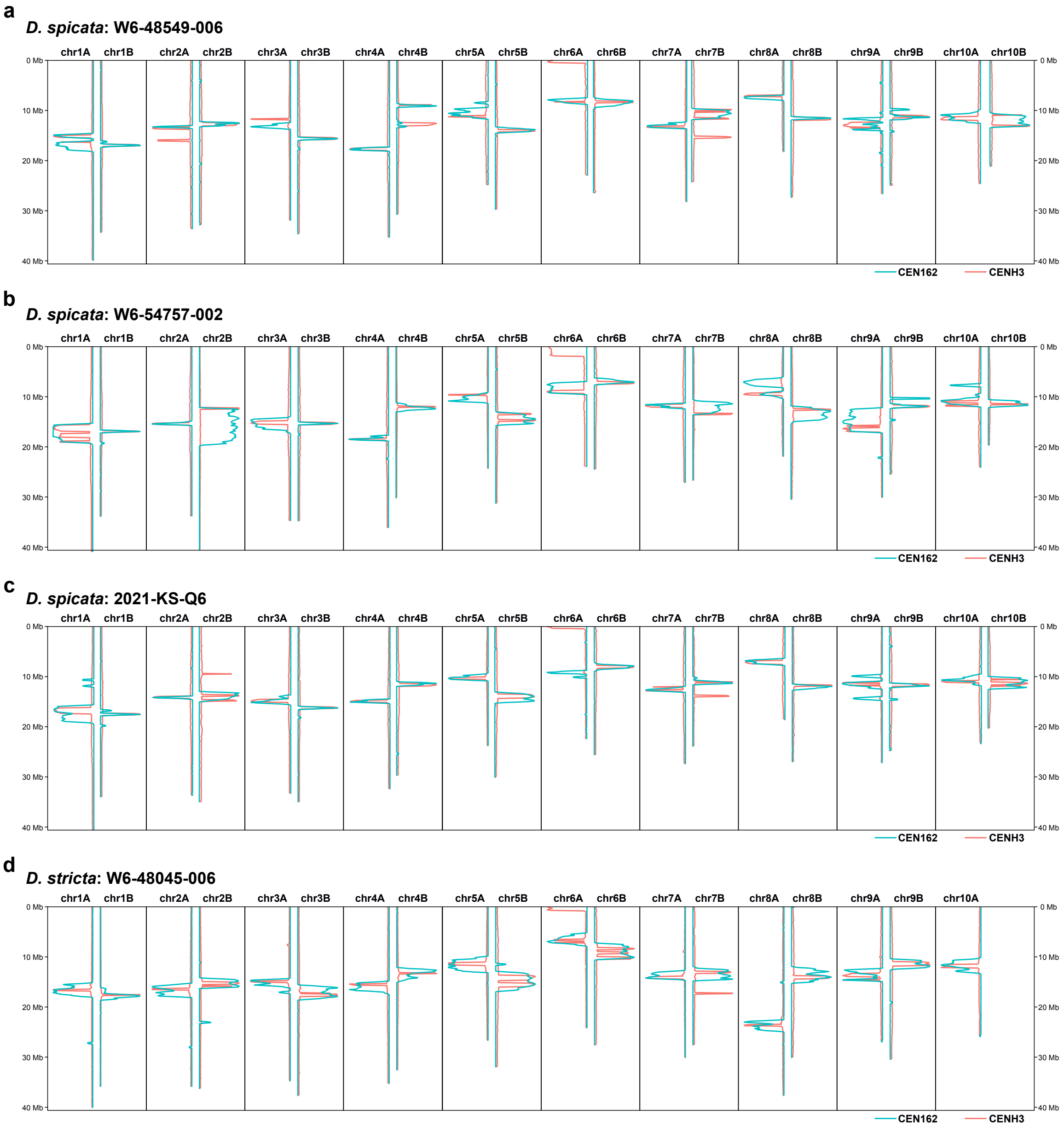

a *D. spicata*: W6-48549-006

b *D. spicata*: W6-54757-002

c *D. spicata*: 2021-KS-Q6

d *D. stricta*: W6-48045-006

Supplementary Figure 1.5: Line plot showing the distribution CEN162 with CENH3 ChIP-seq peaks over each chromosome in *D. spicata*; **a,** W6-54757-002, **b,** W6-54757-002 and **c,** 2021-KS-Q6, and *D. stricta*; **d,** W6-48045-006.

Supplementary Figure 1.6

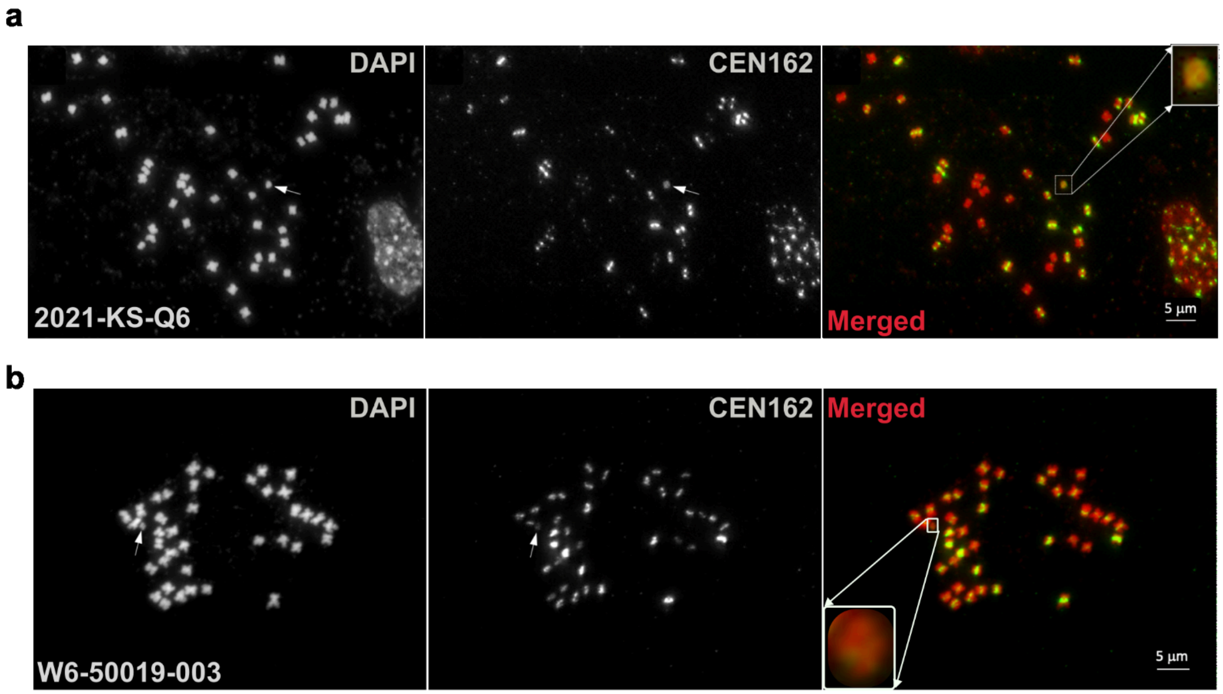

Supplementary Figure 1.6: CEN162 probe used for FISH signal in DAPI-stained metaphase chromosomes, showing one B chromosome in each of the following: **a,** 2021-KS-Q6 and **b,** W6-50019-003.

Supplementary Figure 1.7

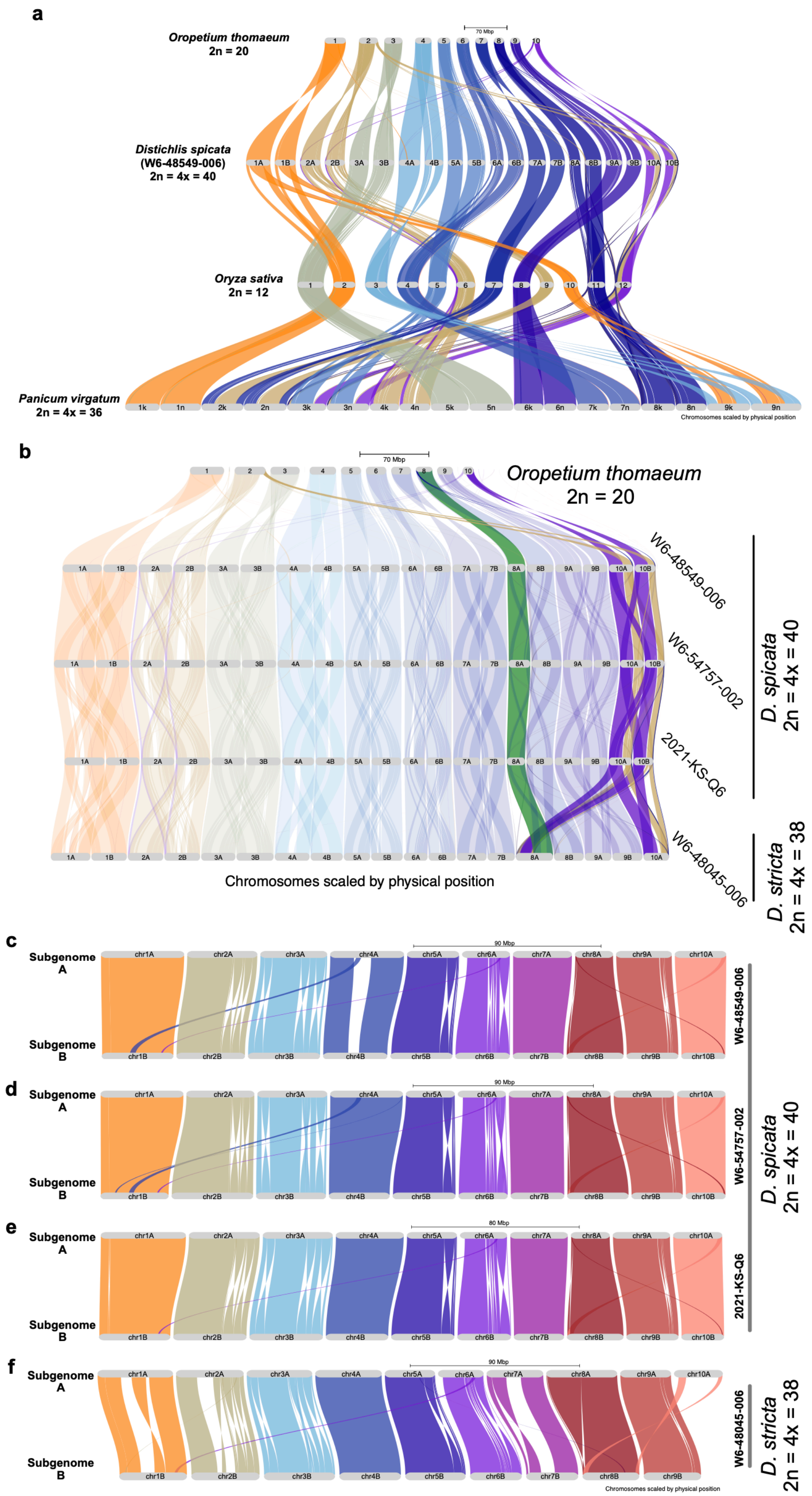

Supplementary Figure 1.7: **a,** Synteny plot of all protein-coding genes among *O. thomaeum*; n = 28930, *D. spicata* (W6-48549-006; n = 67007), *Oryza sativa*; n = 42246 and *Panicum virgatum*; n = 129942. **b,** Synteny plot of all protein-coding genes among *O. thomaeum* and three genets of *D. spicata* (W6-48549-006; n = 67007, W6-54757-002; n = 66946 and 2021-KS-Q6; n = 63604) and one genet of *D. stricta* (W6-48045-006; n = 63870). Chromosome fusion has been highlighted between *D. spicata* (2n = 4x = 40) and *D. stricta* (2n = 4x = 38). Synteny plots between subgenomeA and subgenomeB of all protein coding genes in **c,** W6-48549-006, **d,** W6-54757-002, **e,** 2021-KS-Q6 and **f,** W6-48045-006.

Supplementary Figure 1.8

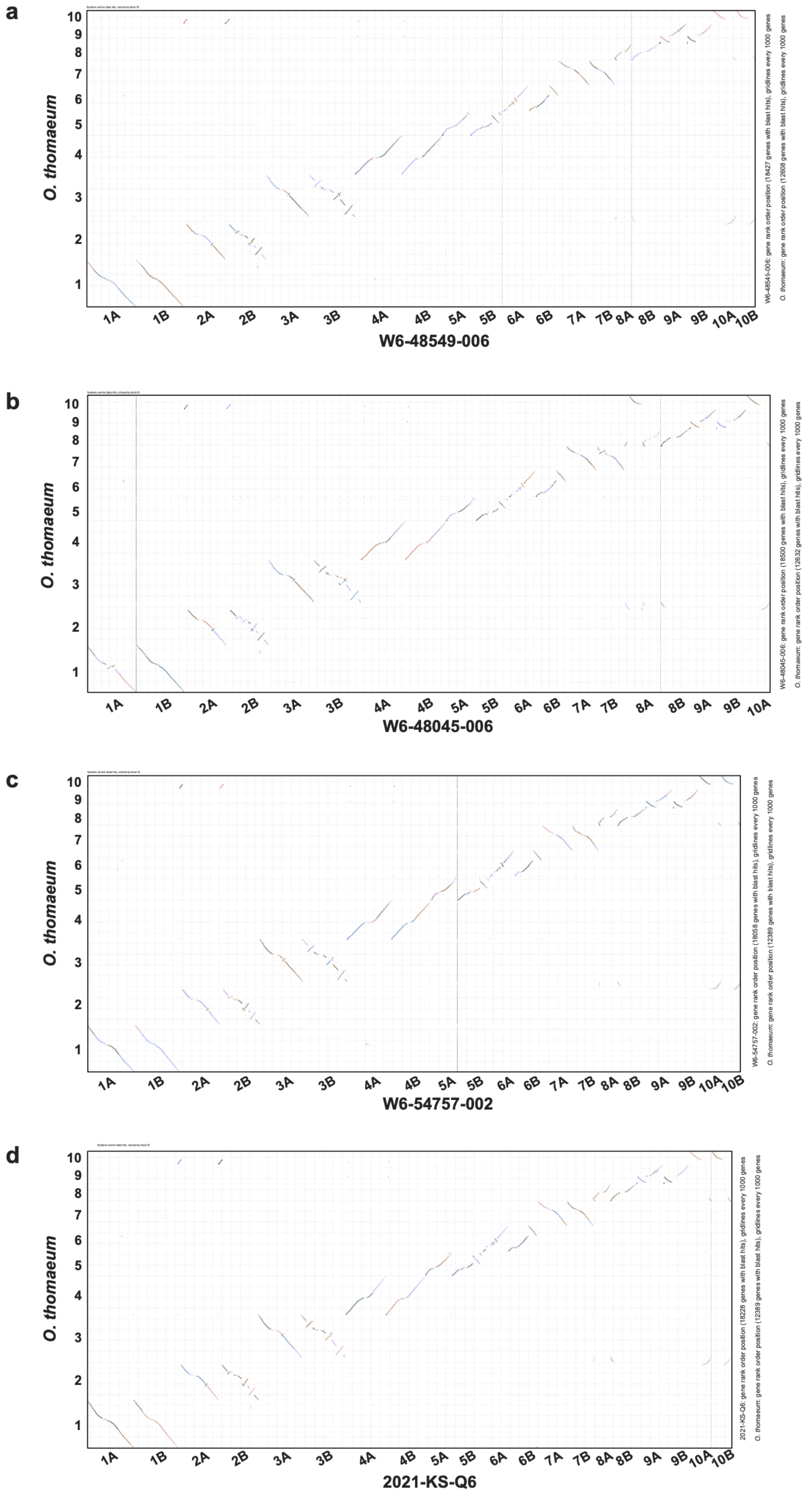

Supplementary Figure 1.8: Syntenic alignments (dotplots) of protein-coding genes among *O. thomaeum* against **a,** W6-48549-006, **b,** W6-48045-006, **c,** W6-54757-002 and **d,** 2021-KS-Q6.

Supplementary Figure 1.9

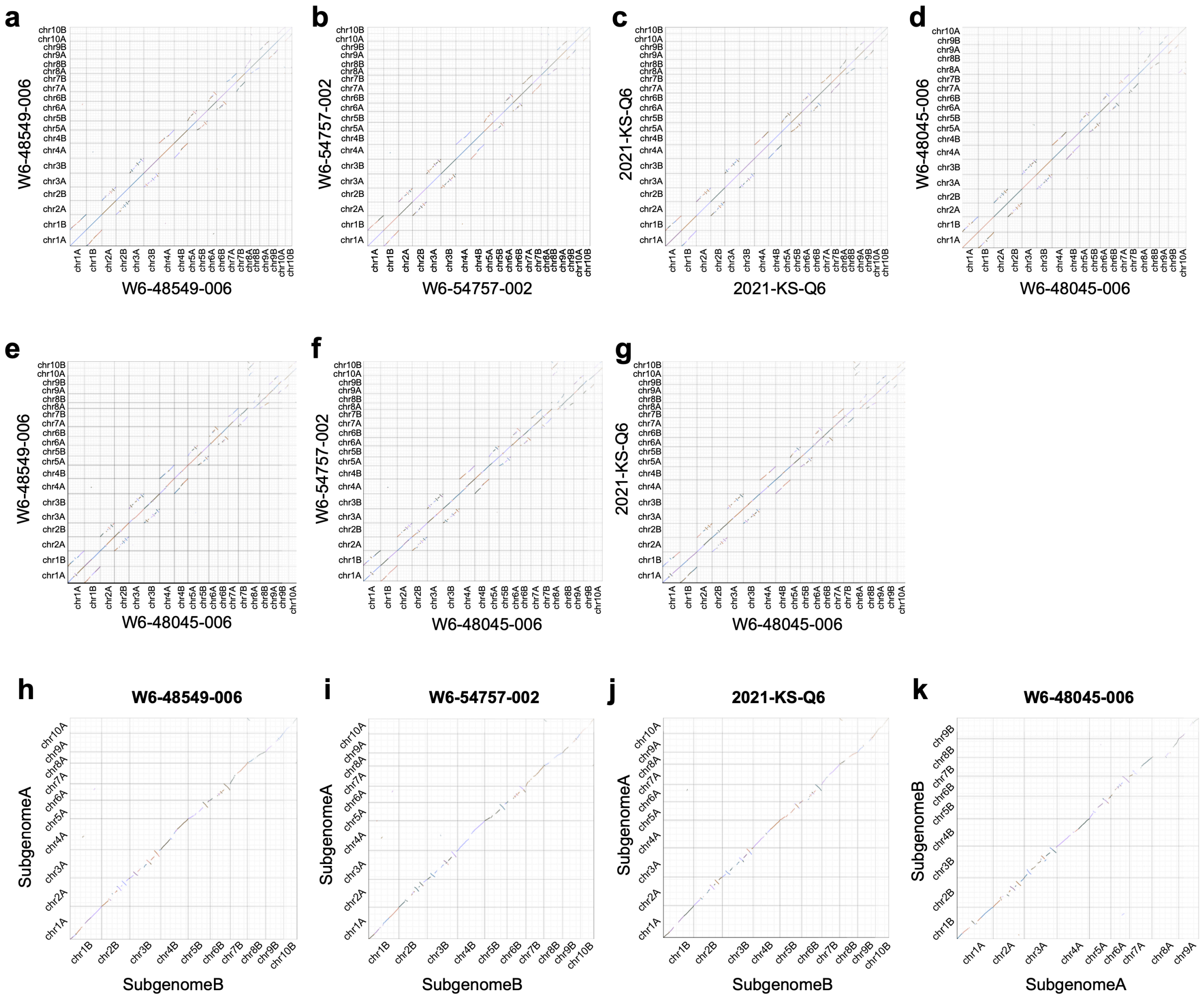

Supplementary Figure 1.9: Self syntenic alignments (dotplots) of protein-coding genes among **a,** W6-48549-006, **b,** W6-54757-002, **c,** 2021-KS-Q6 and **d,** W6-48045-006. Dotplots of *D. stricta* (W6-48045-006) vs *D. spicata* (**e,** W6-48549-006, **f,** W6-54757-002 and **g,** 2021-KS-Q6). Dotplots between subgenomeA and subgenomeB of **h,** W6-48549-006, **i,** W6-54757-002, **j,** 2021-KS-Q6 and **k,** W6-48045-006.

Supplementary Figure 1.10

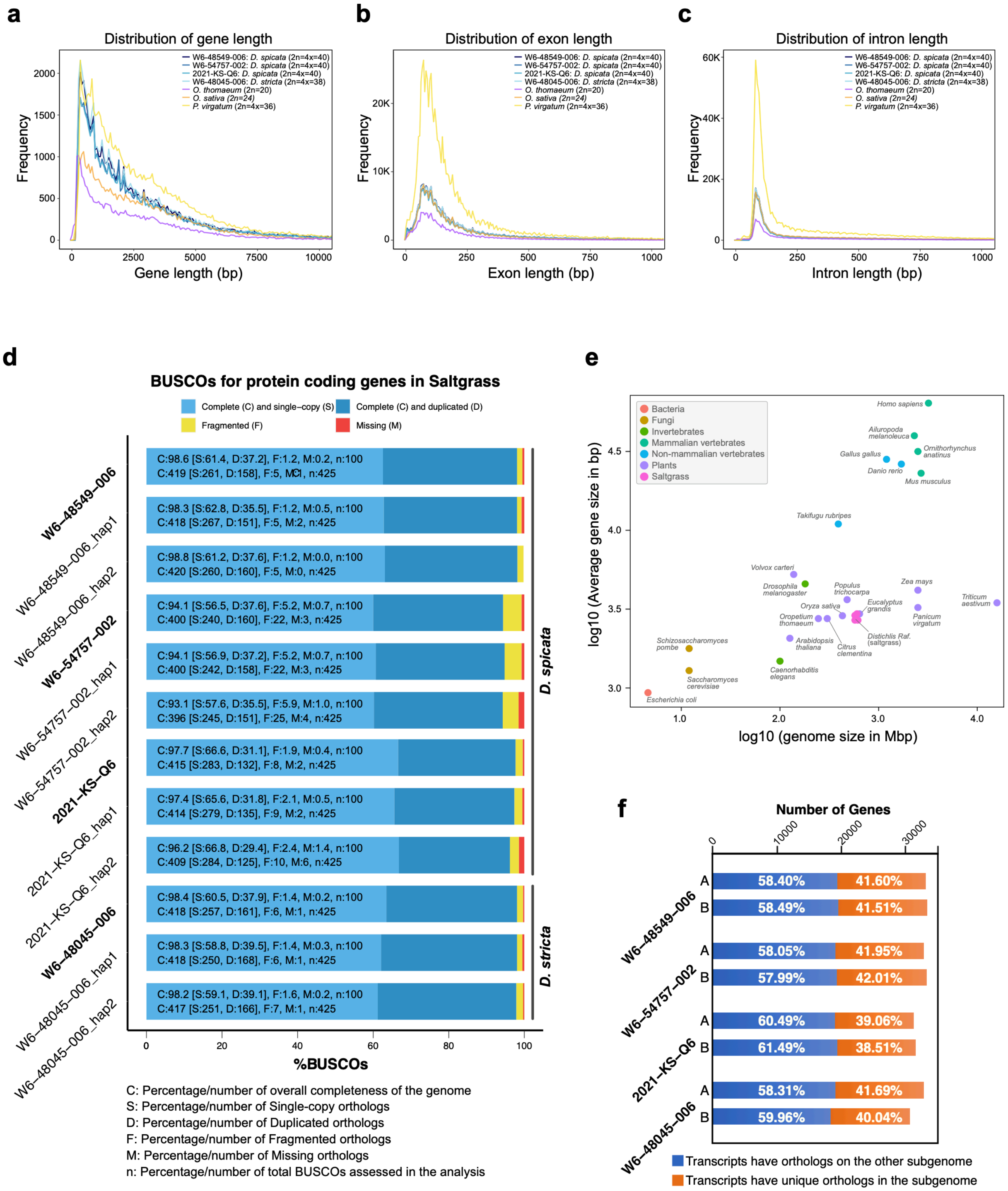

Supplementary Figure 1.10: Length distribution and their comparison of all four genets of saltgrass (W6-48549-006, W6-54757-002, 2021-KS-Q6 and W6-48045-006), *O sativa*, *O. thomaeum* and *P. virgatum* of **a,** genes, **b,** exons and **c,** introns. **d,** BUSCOs for protein-coding genes of all four genets of saltgrass with their two haplotypes. **e,** Genome size vs gene size interpolation of saltgrass and their comparison with other species. **f,** BUSCO categories comparison between subgenomes of all four genets of saltgrass.

Supplementary Figure 1.11

a

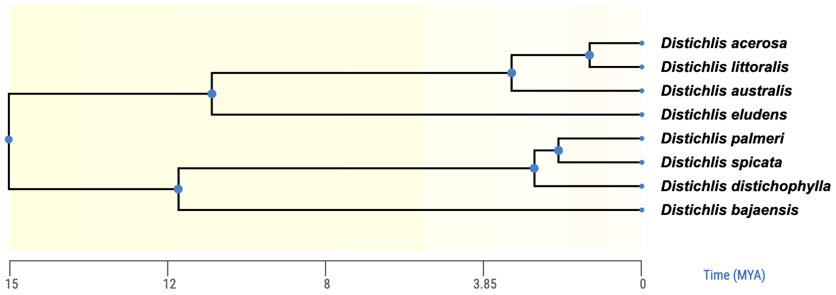

Supplementary Figure 1.11: Timetree was built from eight saltgrass species based on their plasmid and mitochondria from https://timetree.org/ database.

Supplementary Figure 2.1

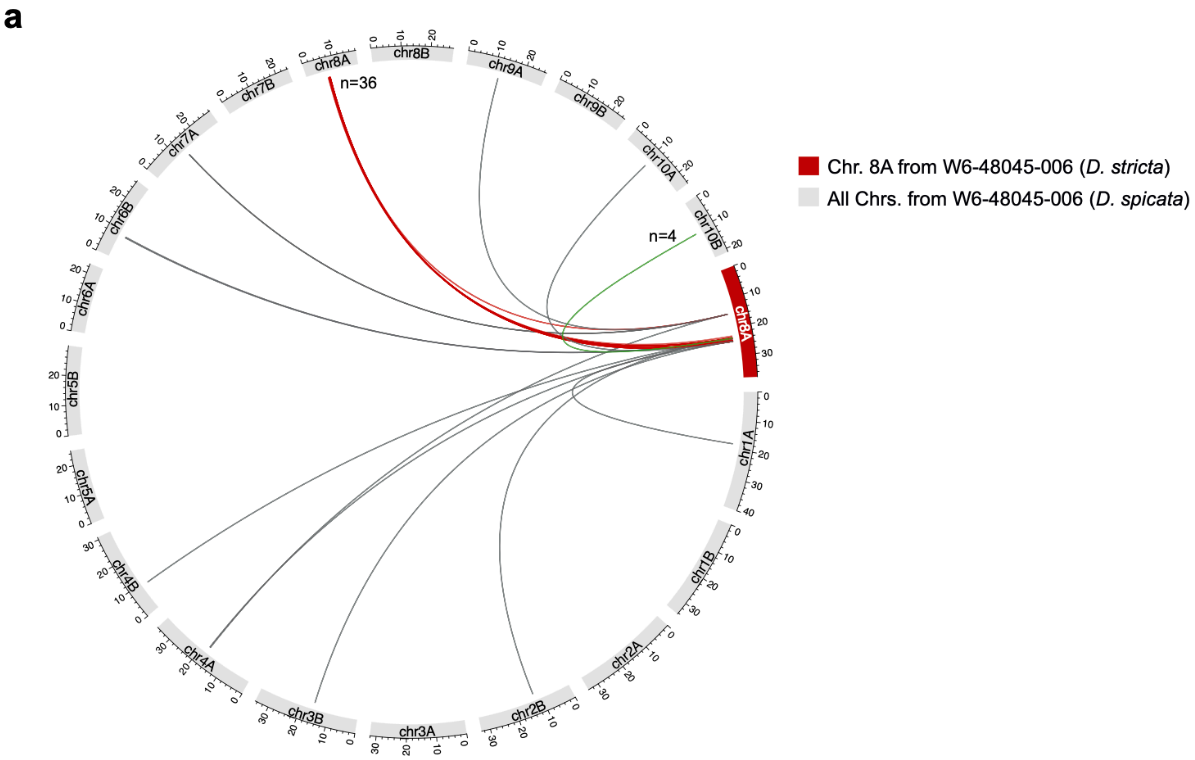

Supplementary Figure 2.1: Synteny analysis of CEN162 on the fused Chr. 8A of *D. stricta* shows that the highest amount of CEN162 (represented by 'n') is shared with Chr. 8A, and the second highest amount is shared Chr. 10B of *D. spicata*.

Supplementary Figure 3.1

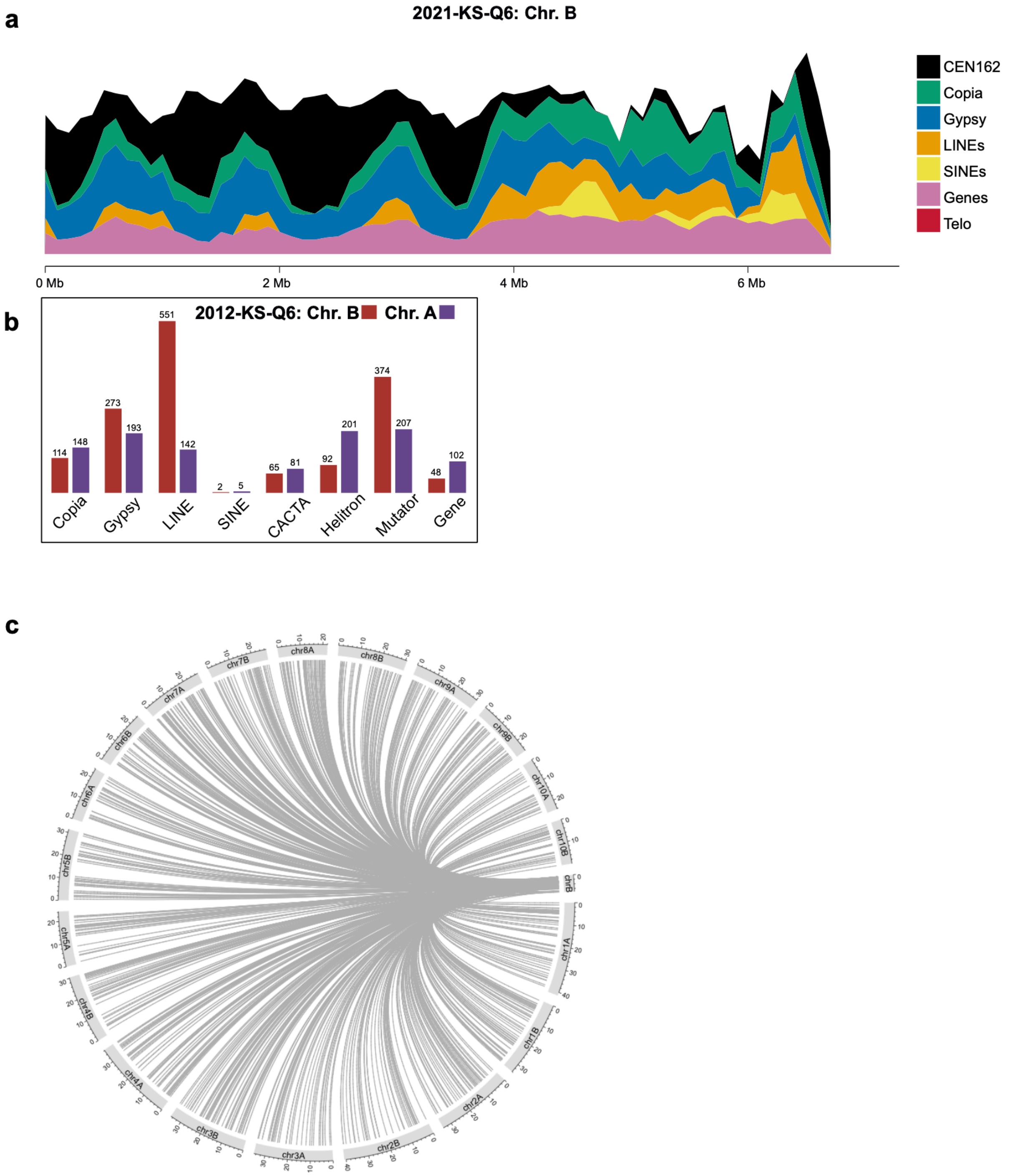

Supplementary Figure 3.1: Distribution of different repetitive elements (CEN162, *Copia*, *Gypsy*, LINEs, SINEs), genes and telomere on the B chromosome of 2021-KS-Q6 across 300 Kb bins. **b,** Comparisons of distribution patterns of repetitive elements (*Copia*, *Gypsy*, LINEs, SINEs, CACTA, Helitron, Mutator) and genes between B and A chromosomes (normalized over 1 Mb) in 2021-KS-Q6. **c,** Repeat elements from Chr. B synteny from all Chrs. A in W6-54757-006.

Supplementary Figure 3.2

a 2n=4x=***40+1B***; 2021-KS-Q13; *D. spicata*

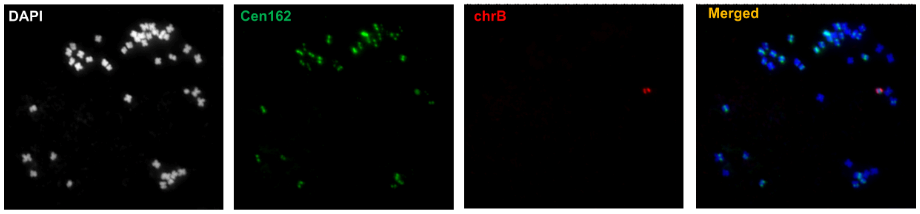

b 2n=4x=***40+2B***; W6-54695-001; *D. spicata*

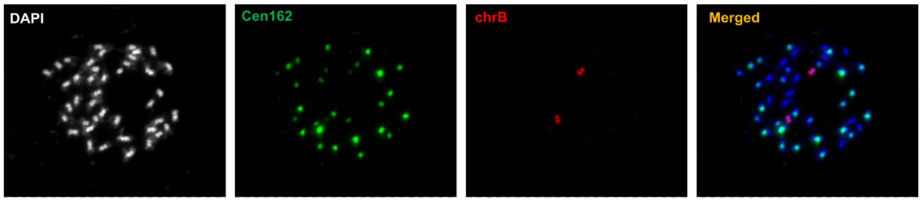

c 2n=4x=***40+3B***; W6-54695-002; *D. spicata*

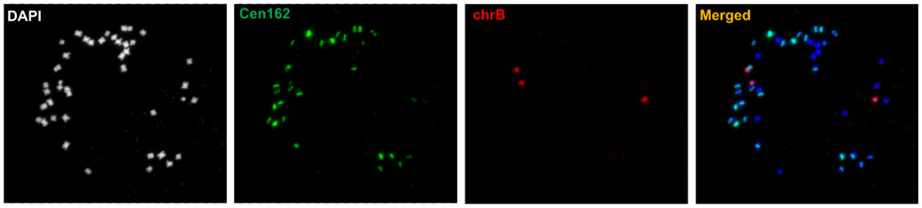

d 2n=4x=***40+1B***; 2021-KS-Q6; *D. spicata*

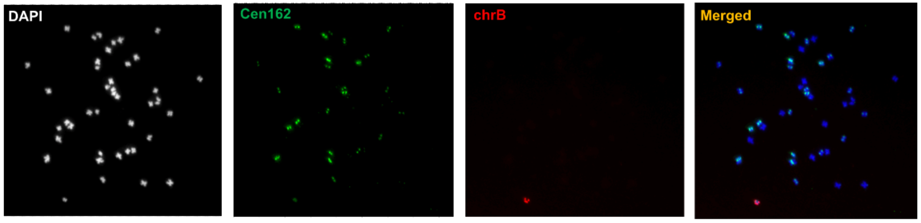

e 2n=4x=***40+2B***; Granite2018; Plant #4 *D. spicata*

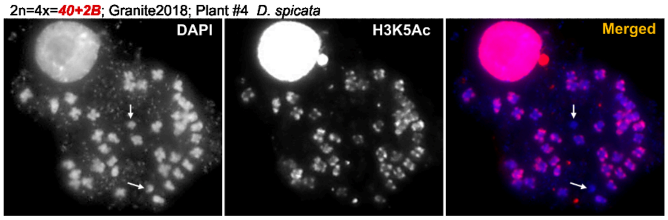

f 2n=4x=***40+3B***; Granite2018; Plant #5 *D. spicata*

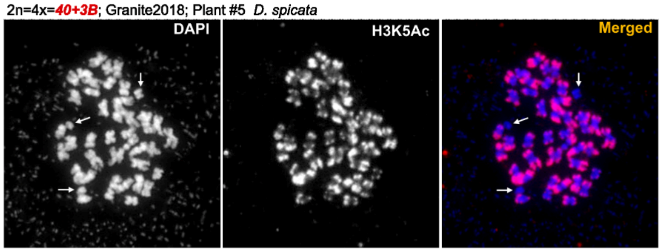

g 2n=4x=***40+2B***; Granite2018; Plant #6 *D. spicata*

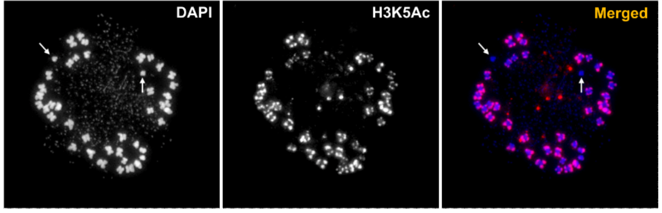

Supplementary Figure 3.2: DAPI stain showing one, two, and three B chromosomes were observed in **a,** 2021-KS-Q13; **b,** W6-54695-001; **c,** W6-54695-002; and **d,** 2021-KS-Q6 saltgrass genets, respectively. FISH utilized saltgrass centromere (CEN162) probes depicted in green, while Chr. B probes were shown in red. H3K5Ac ChIP data are illustrated for all A chromosomes but not for the B chromosomes in three plants of the Granite 2018 population, with **(e)** two, **(f)** three, and **(g)** two Chrs. B.

Supplementary Figure 3.3

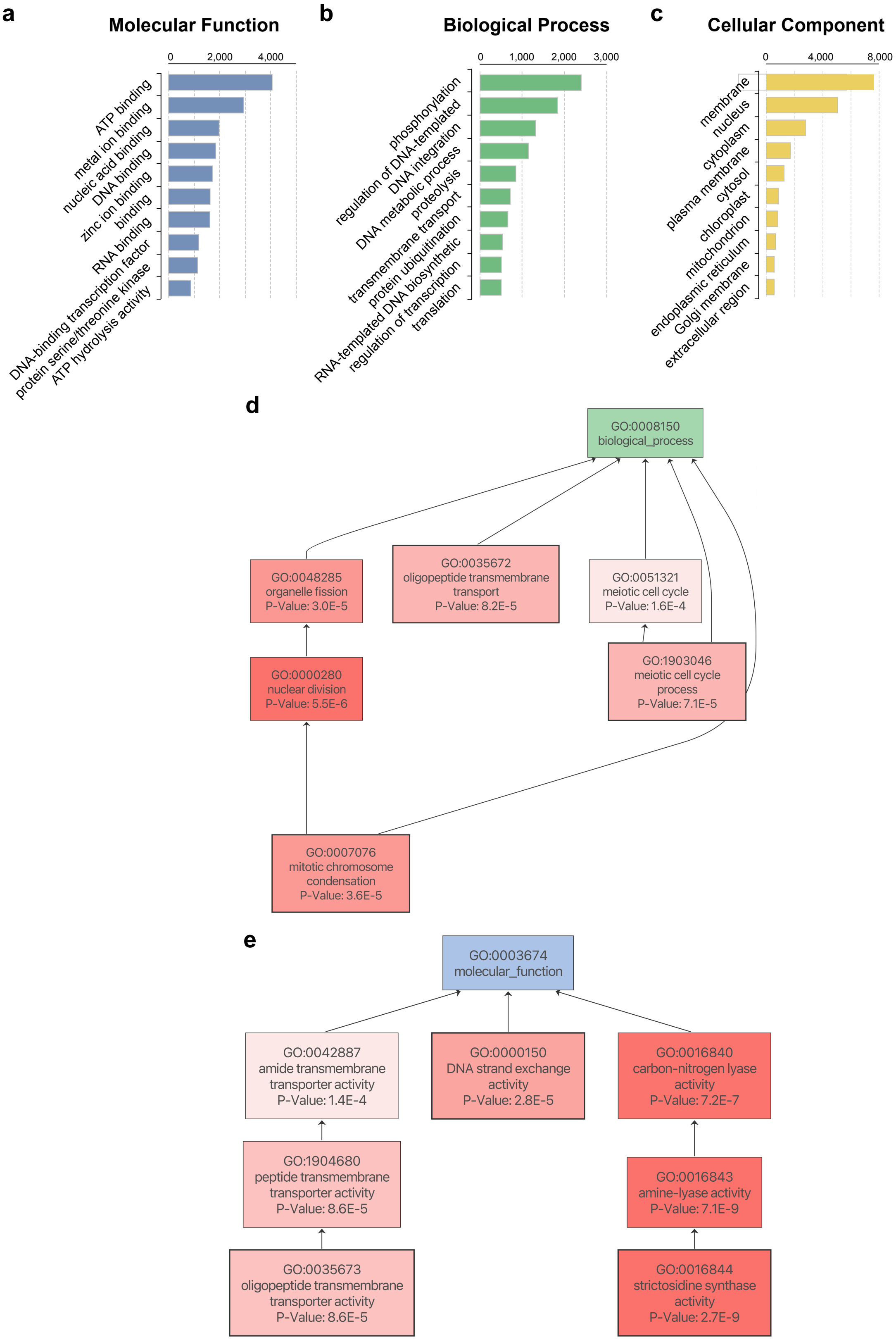

Supplementary Figure 3.3: Top 10 counts of **a,** Molecular Function, **b,** Biological Process, and **c,** Cellular Component Gene Ontology (GO) categories are depicted for the protein-coding genes located on

Chromosome B of W6-48549-006. The combined graph illustrates the GO category distribution with corresponding p-values for **d,** Biological Process and **e,** Molecular Function.

Supplementary Figure 4.1

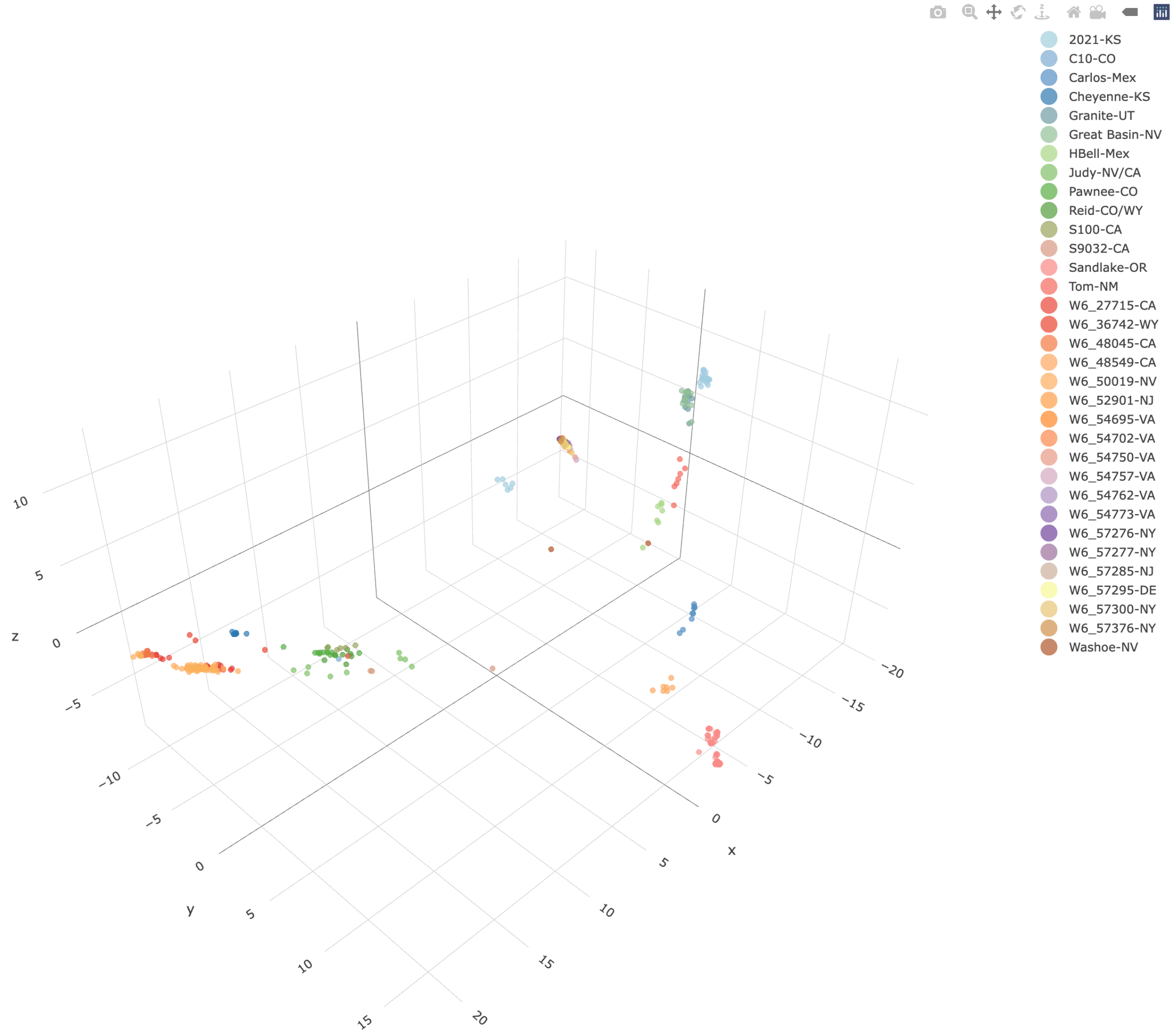

Hyperlink for the interactive 3D PCA plot
https://kashiff007.github.io/SFig.4.1/

Supplementary Figure 4.1: Three-dimensional PCA plot depicting 364 saltgrass samples, with the first three principal components represented along the x, y, and z axes, respectively (https://kashiff007.github.io/SFig.4.1/).

Supplementary Figure 4.2

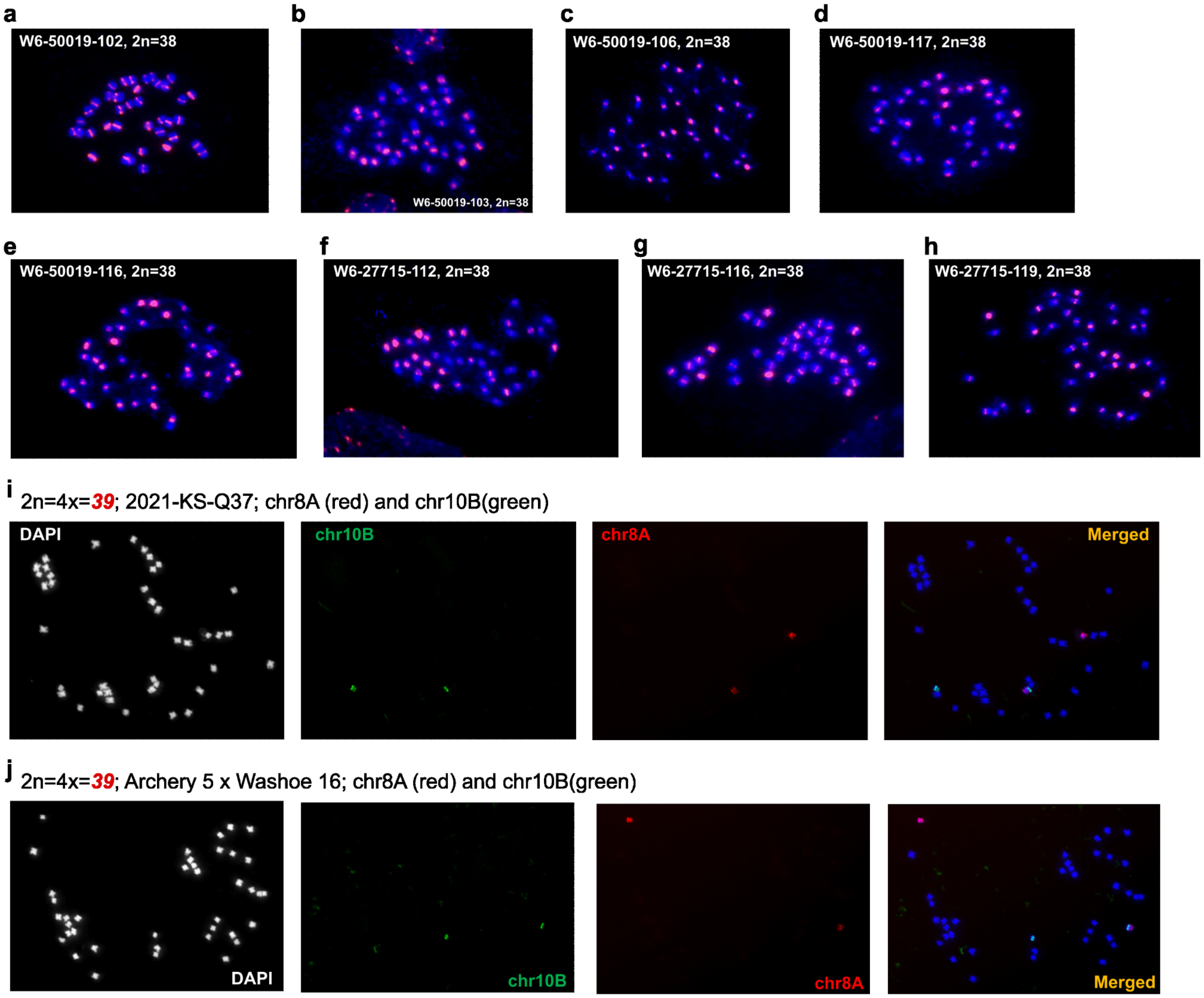

Supplementary Figure 4.2: Cytogenetic report featuring CEN162 probe FISH from W6-49549-006 of *D. stricta* (**a-h**) depicting various hybrid genets: W6-50019-102, W6-50019-103, W6-50019-106, W6-50019-117, W6-50019-116, W6-27715-112, W6-27715-116, and W6-27715-119, all exhibiting a consistent chromosome count of 2n=38. **i,** Notably, genotype 2021-KS-Q37, with 39 chromosomes, displays an incomplete fusion with Chr. 10B probe FISH labelled in green and Chr. 8A in red, elucidating the hybridization event between *D. spicata* and *D. stricta*. **j,** Hand-pollinated hybrids between *D. spicata* and *D. stricta* resulted in the hybrid Archery 5 x Washoe 16 (2n=39). Chromosomal analysis using probes specific to Chr. 10B (green) and Chr. 8A (red) confirmed the presence and integration of these chromosomes in the hybrid genome.

Supplementary Figure 4.3

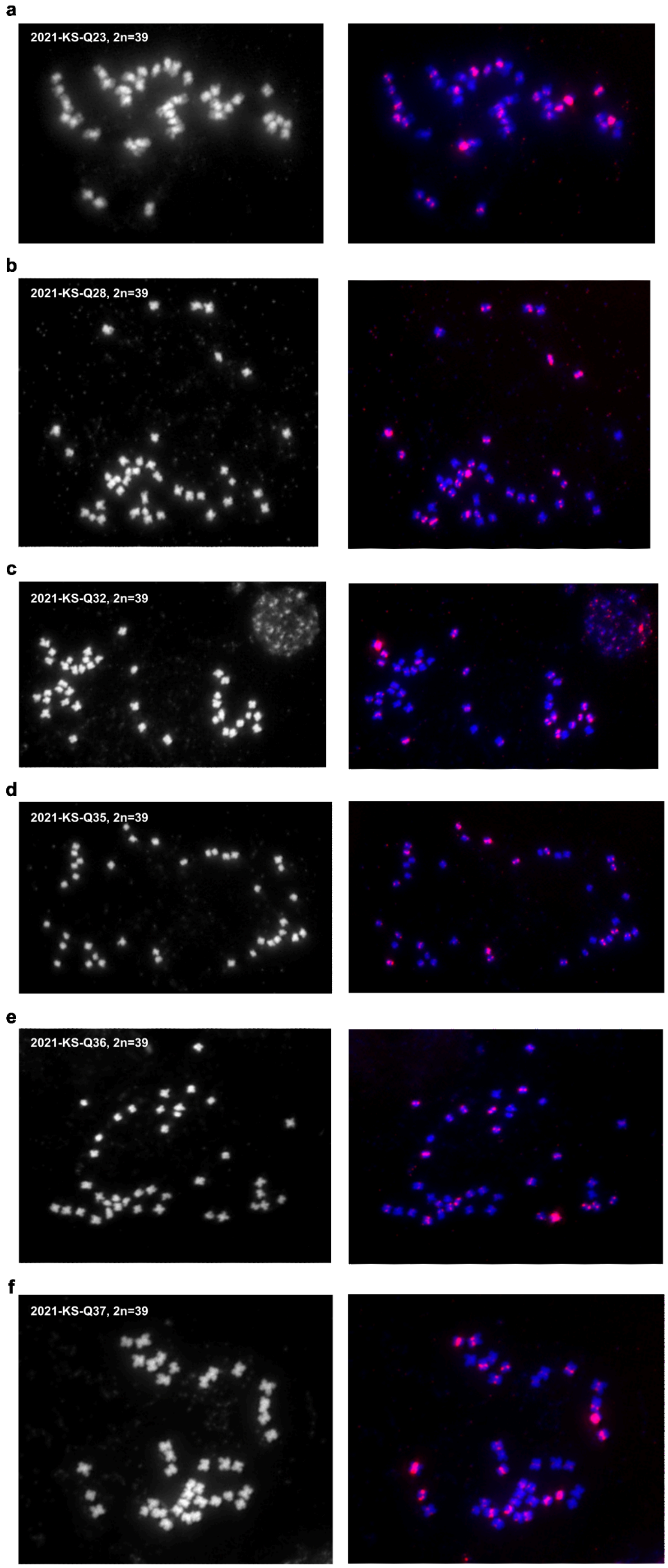

Supplementary Figure 4.3: **a-f:** Cytogenetic analysis depicts six genets from Kansas (2021-KS-Q23, 2021-KS-Q28, 2021-KS-Q32, 2021-KS-Q35, 2021-KS-Q36 and 2021-KS-Q37) exhibiting hybridization between *D. spicata* and *D. stricta* using the CEN162 probe from W6-49549-006, revealing a total of 39 chromosomes in each genet.

Supplementary Figure 5.1

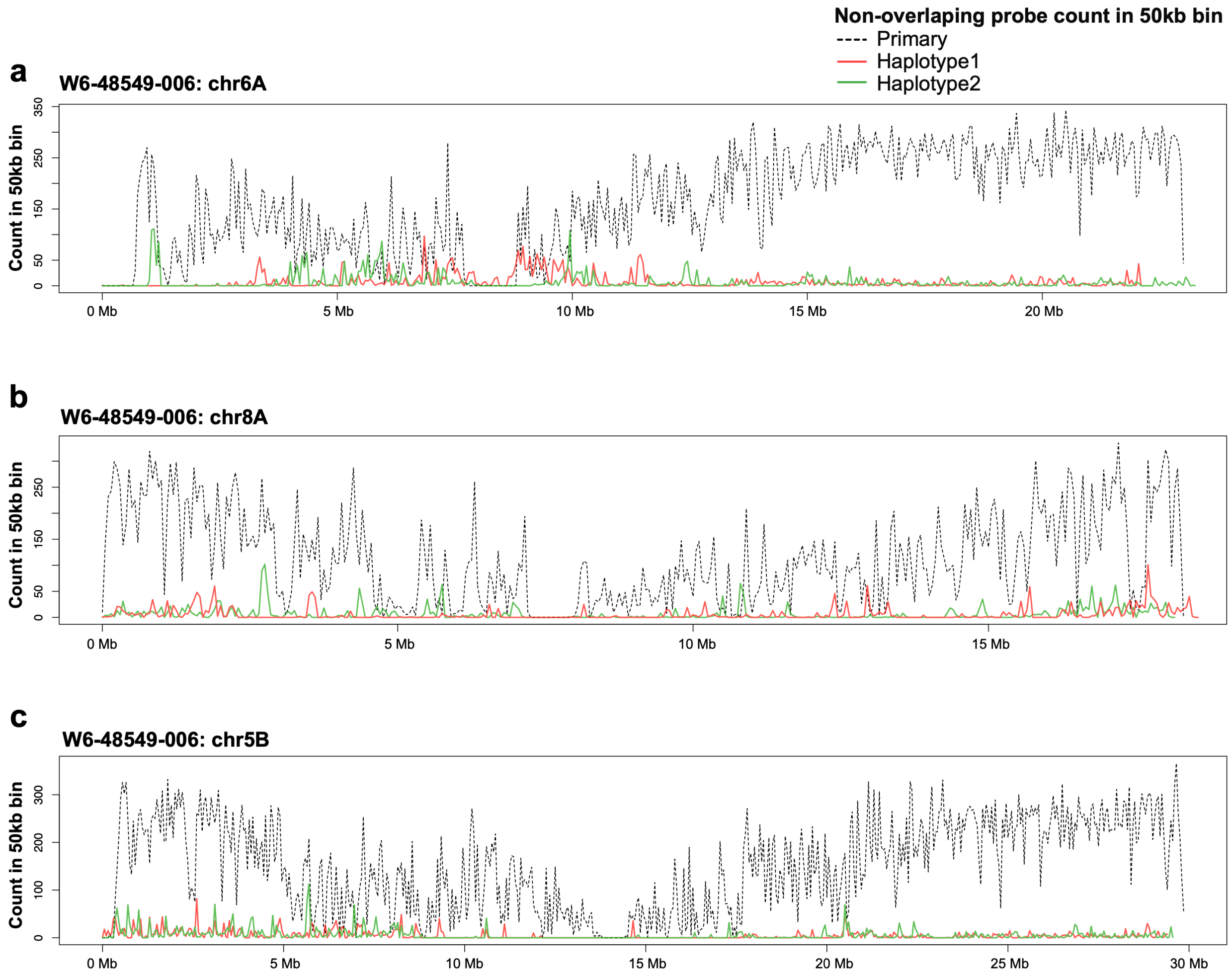

Supplementary Figure 5.1: Line plot depicting non-overlapping probe counts derived from the female-specific genomic region across the chromosomes **a,** 6A, **b,** 8A, and **c,** 5B. Each data point represents a 50 Kb bin and is displayed for the primary chromosome (dashed line), haplotype 1 (in red), and haplotype 2 (in green) of the W6-48549-006 genotype.

Supplementary Figure 5.2

a SDR (red); W6-48045-006; *D. stricta*

b SDR (red); 2021-KS-Q6; *D. spicata*

Supplementary Figure 5.2: FISH analysis depicting DAPI-stained chromosomes from **a,** *D. stricta* (W6-48045-006) and **b,** *D. spicata* (2021-KS-Q6), highlighting the Sex Determining Region (SDR) in red. The probes utilized are derived from a genomic region specific to females.

Supplementary Figure 5.3

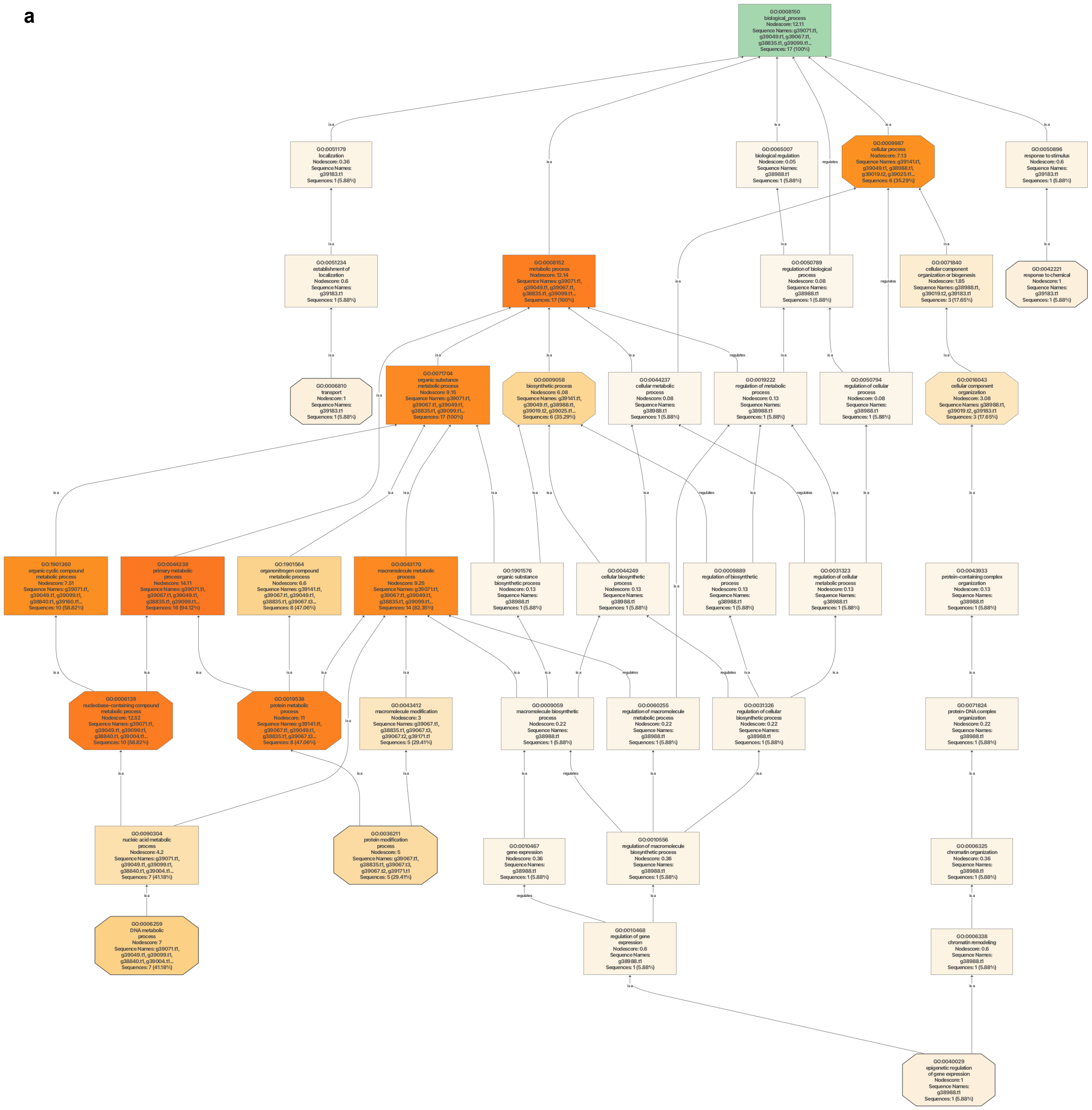

Supplementary Figure 5.3: **a,** A combined biological process Gene Ontology (GO) chart depicting the distribution of 40 transcripts from SDR, where female-specific k-mers were mapped (sex-associated genes).
]